Periodica Polytechnica Chemical Engineering, 69(4), pp. 720–734, 2025

Modeling and Experimental Study of Liquid–liquid Extraction of Water + Formic Acid + 1-Octanol with NaCl and KCl Using Non-random Two-liquid and Artificial Neural Network Models

Djemoui Laiadi[1,2], Khaled Athmani[1,2*], Chaker Laiadi[3], Abdelmalek Hasseine[1,2], Abdelkrim Merzougui[1,2], Elhachmi Guettaf Temam[4]

[1] Laboratory of LAR-GHYDE, University of Biskra, 07000 Biskra, P.O.B. 145 RP, Algeria
[2] Chemical and Environmental Process Engineering Laboratory, University of Biskra, 07000 Biskra, P.O.B. 145 RP, Algeria
[3] Department of Pharmaceutical Engineering, Faculty of Process Engineering, University Constantine 3 Salah Boubnider, 25000 El Khroub, P.O.B. 72, Algeria
[4] Physics Laboratory of Thin Films and Applications, University of Biskra, 07000 Biskra, P.O.B. 145 RP, Algeria
[*] Corresponding author, e-mail: khaled.athmani@univ-biskra.dz

Received: 16 September 2025, Accepted: 18 November 2025, Published online: 28 November 2025

Abstract

This study investigates the liquid–liquid extraction behavior of a ternary system composed of water, formic acid, and 1-octanol in the presence of inorganic salts (NaCl and KCl) at varying concentrations of 0%, 5%, 10%, and 15%. Each salt was examined individually to assess its impact on the extraction efficiency. Experimental solubility data and tie-line compositions were obtained. The results demonstrate that the addition of salt significantly improves the efficiency of extraction. NaCl was found to induce a stronger salting-out effect than KCl, especially at 10% concentration, where the highest selectivity and distribution coefficient were observed. To model the phase behavior, both the Non-Random Two-Liquid (NRTL) thermodynamic model and an Artificial Neural Network (ANN) were employed based on the experimental results. A Neural Architecture Search approach was implemented to optimize ANN structure. Both models exhibited strong predictive capability; however, the ANN model demonstrated superior performance, achieving higher accuracy and lower prediction errors than the NRTL model, particularly at high salt concentrations.

Keywords

Artificial Neural Network, liquid–liquid equilibrium, NRTL, Neural Architecture Search, salting effect

1 Introduction

Liquid–liquid extraction (LLEx) is a well-established separation technique that exploits the differential solubility of compounds in immiscible liquid phases. It is particularly well-suited for systems where traditional separation methods, such as distillation or adsorption, are limited due to low volatility or thermal sensitivity of the target compounds [1, 2].

Formic acid (FA), a promising carrier for hydrogen and carbon monoxide, is difficult to separate from water due to strong molecular interactions and azeotrope formation. LLEx offers an energy-efficient alternative to distillation for recovering dilute FA solutions. Laitinen et al. [3] investigated the use of 2-methyltetrahydrofuran (2-MTHF) as an extractant to separate FA from aqueous streams originating from CO_2 electroreduction.

1-Octanol is widely employed in reactive liquid-liquid extraction for separating FA from aqueous streams due to its moderate polarity, hydrogen-bonding capacity, and synergistic effects with extractants like tri-n-octylamine (TOA) [4]. Senol [5] conducted experimental investigations on the ternary mixture water + FA + 1-octanol, providing valuable phase equilibrium data and insights into the extraction mechanisms. Senol [5] measured binodal curves and tie-line compositions at 293.15 K and 101.3 kPa, observing significant distribution of FA into the octanol-rich phase due to hydrogen bonding interactions. The study applied a solvatochromic-UNIFAC model (SERLAS), which captured the equilibrium behavior with a mean error of ~28%. The solubility and tie-line data for the ternary systems (water + FA + aliphatic alcohols) were experimentally determined at T = 298.2 K and atmospheric pressure using four primary alcohols: 1-butanol, 1-pentanol, 1-hexanol, and 1-heptanol [6]. All systems exhibited Type-1

Cite this article as: Laiadi, D., Athmani, K., Laiadi, C., Hasseine, A., Merzougui, A., Guettaf Temam, E. "Modeling and experimental study of Liquid–liquid Extraction of Water + Formic Acid + 1-Octanol with NaCl and KCl Using Non-random Two-liquid and Artificial Neural Network Models", Periodica Polytechnica Chemical Engineering, 69(4), pp. 720–734, 2025. https://doi.org/10.3311/PPch.42242

liquid-liquid equilibrium (LLEq) behavior, with the largest immiscibility region observed for 1-heptanol.

The addition of salts to aqueous systems can significantly influence phase behavior through the salting-out effect. This phenomenon reduces the solubility of organic solutes in the aqueous phase by altering the solvent structure and reducing water's capacity to solvate polar molecules, thereby enhancing the partitioning of solutes like FA into the organic phase [7, 8]. Several studies have demonstrated that electrolytes improve phase separation and increase distribution coefficient (D_2) in LLEq systems, making salt addition a practical method for optimizing extraction efficiency [9]. Fu et al. [10] investigated the salting-out extraction of carboxylic acids – including formic, acetic, lactic, and citric acids using a biphasic system composed of ethanol and ammonium sulfate. The study found that extraction efficiency improved with increasing acid hydrophobicity, indicating that both molecular characteristics and system parameters play a critical role in governing phase separation and solute distribution.

To design and scale up LLEq systems effectively, accurate prediction of phase behavior is required. Thermodynamic models such as the Non-Random Two-Liquid (NRTL) model are widely used to describe non-ideal interactions in liquid mixtures [11, 12]. These models provide valuable insights into activity coefficients and allow for the estimation of tie-line compositions and D_2. However, they often rely on regression against experimental data and may have limited generalizability outside calibrated systems.

As an alternative or complement to classical thermodynamic models, machine learning techniques particularly Artificial Neural Networks (ANNs) have emerged as powerful tools in process modeling [13–15]. ANNs are capable of capturing complex nonlinear relationships without requiring explicit knowledge of the underlying physical laws. By learning directly from experimental data, these models offer flexibility and predictive power, making them suitable for systems with intricate or poorly understood interactions. To further enhance the performance and generalization of ANN models, this study employed a Neural Architecture Search (NAS) strategy. NAS automatically identifies the optimal network configuration by systematically exploring combinations of key hyperparameters such as the number of neurons in each hidden layer and the type of activation functions [16, 17].

ANNs have been increasingly applied in liquid–liquid equilibrium studies as a data-driven alternative to traditional thermodynamic models [18–21]. Their ability to model nonlinear and complex phase behavior directly from experimental data makes them well-suited for systems involving salting-out effects, highly non-ideal interactions, or multicomponent mixtures. Moghadam and Asgharzadeh [22] investigated the application of ANNs for modeling liquid–liquid equilibrium in ternary systems, including water + propionic acid + diethyl phthalate, water + propionic acid + dodecanol, and water + butyric acid + dodecanol. They compared multilayer backpropagation and Group Method of Data Handling (GMDH)-type networks, showing that ANNs effectively simulate LLEq behavior across compositions and temperatures, outperforming solvatochromic polarity-based methods. A custom tool, FeedGen, was developed to generate training data. Argatov and Kocherbitov [23] proposed two ANN-based thermodynamic models were proposed to predict vapor–liquid equilibrium (VLE) in multicomponent systems, serving as generalizations of the Wilson and NRTL models. A hybrid model combining ANNs with the NRTL framework was also introduced, using neural networks to estimate the excess Gibbs energy and derive activity coefficients. The models were tested on systems such as acetic acid + n-propyl alcohol + water at 313.15 K, demonstrating improved accuracy over traditional approaches. Laiadi et al. [24] applied an ANN and a modified extended-UNIQUAC model to correlate LLEq data for the water + 2-butanone + salt system. Their study demonstrated that while both models could represent the experimental data, the ANN model achieved significantly lower prediction errors, highlighting its superior ability to capture nonlinear interactions in electrolyte-containing systems.

The primary objective of this study is to investigate the influence of NaCl and KCl on the extraction behavior of FA from aqueous solutions into 1-octanol, and to evaluate the performance of both classical (NRTL) and ANN models in predicting the phase behavior across varying salt concentrations. The work aims to provide insights into the optimization of electrolyte-assisted LLEx processes through a combined experimental and modeling framework.

2 Experimental

2.1 Materials

All chemicals used in this study were of analytical grade and employed without further purification. FA (purity 98%), 1-octanol (98.5%), sodium chloride (99.5%), and potassium chloride (99.5%) were purchased from Biochem Chemopharma. Distilled water was obtained from the laboratory supply. These substances were selected based on their compatibility with the target extraction system and

their well-known physical properties. The refractive indices of the pure components at 293.15 K and 291.15 K are summarized in Table 1 [25].

2.2 Apparatus and procedure

2.2.1 Binodal curve determination (solubility isotherm)

The binodal curve was determined using the cloud point titration method [26–28] at a temperature of 293.15 ± 0.1 K. Refractive index measurements (Princeton Instruments (PI) model 2WAJ with $\pm 10^{-4}$ precision) were used to calibrate the compositions of the coexisting phases. The curve was constructed in two parts.

2.2.2 Right-hand side of the binodal curve

Binary mixtures of the diluent (1-octanol) and solute (FA or lactic acid) were prepared by mass using a Nahita model 5034/200 electronic balance with an accuracy of ±0.0001 g. These mixtures were stirred using a constant-speed mechanical stirrer, and the solvent (water) was gradually added dropwise until turbidity appeared, indicating the onset of phase separation. At this point, the volume of water added was recorded, and the refractive index of the resulting mixture was measured using an Abbe refractometer. The maximum error in the calculated mass fractions was estimated to be less than 0.0002 [28].

2.2.3 Left-hand side of the binodal curve

The same steps were repeated, but the initial binary mixtures were prepared using solute and solvent. The diluent was then added gradually until the onset of turbidity, and the refractive index was recorded in the same manner.

2.2.4 Tie-line construction

The tie-lines were determined by preparing a series of ternary mixtures (diluent + solute + solvent) of total mass 20 g with varying compositions. Each mixture was vigorously stirred at room temperature using a magnetic stirrer for 2 h to ensure thorough mixing. The systems were then left to settle in 100 mL separatory funnels for 24 h to reach equilibrium. After phase separation by decantation, the extract and raffinate phases were individually weighed, and samples from each phase were taken for refractive index measurement using a refractometer. These measurements were used to calculate the equilibrium compositions of both phases [29].

Table 1 Measured and reported refractive indices of selected chemicals at 293.15 K

Chemical	Refractive index at 293.15 K	
	Experimental	Dean [25]
Water	1.334	1.333
1-octanol	1.4280	1.4290
FA	1.3714	1.3704

3 Results and discussion

To present this study clearly, Section 3 is divided into three parts.

3.1 Experimental results

This section presents the experimental findings obtained for the ternary system water + FA + 1-octanol. The results are systematically organized into four subsections to highlight the key aspects of the extraction process. First, the solubility isotherms are discussed, illustrating the phase behavior and equilibrium compositions of the system at constant temperature. Second, selectivity (S) values are evaluated to determine the separation efficiency of 1-octanol for FA relative to water. Third, D_2 are calculated to quantify the partitioning of FA between the aqueous and organic phases. Finally, the reliability of the experimental data is assessed through consistency tests and analytical accuracy, ensuring the validity of the obtained results for further modeling and comparison.

3.1.1 Binodal curve

This section describes the determination of the binodal curves for the ternary system. The experimental procedure used to identify the equilibrium compositions of the coexisting phases is outlined, and the data are used to construct the binodal curve.

Fig. 1 shows the solubility isotherms for the quaternary system water + formic acid + 1-octanol + NaCl at varying concentrations (0%, 5%, 10%, and 15%). As NaCl concentration increases, a clear salting-out effect is observed. This phenomenon reduces the solubility of FA in the aqueous phase, leading to enhanced separation between the organic and aqueous phases.

Fig. 2 illustrates a similar analysis for water + FA + 1-octanol + KCl. While the general trend of reduced solubility persists with increasing KCl concentration, the salting-out effect is less pronounced than with NaCl. This difference is attributed to the ionic strength and hydration properties of Na+ *vs*. K+ ions. The presence of salt alters the chemical potential and activity coefficients in the system. NaCl, due to its stronger ionic interactions, exerts a higher influence on phase separation compared to KCl. These results are consistent with previous literature on salting-out behavior in liquid-liquid systems.

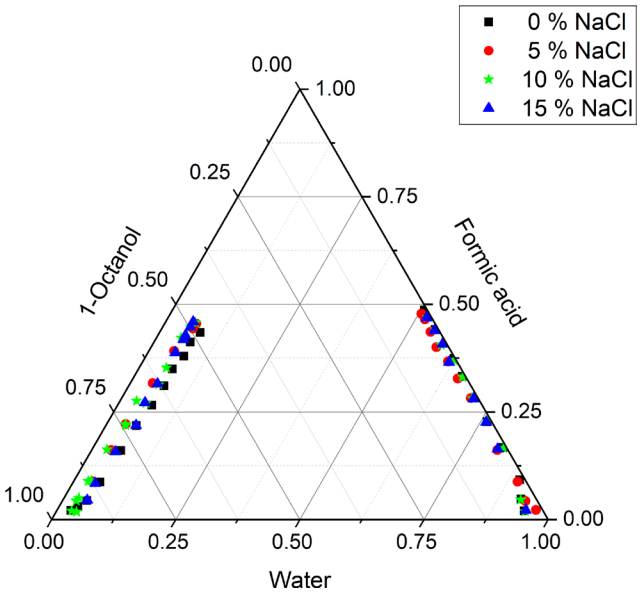

Fig. 1 Binodal curves for the system water + formic acid + 1-octanol + NaCl at $T = 293.15$ K and atmospheric pressure for different NaCl weight percentages (0%, 5%, 10%, and 15%)

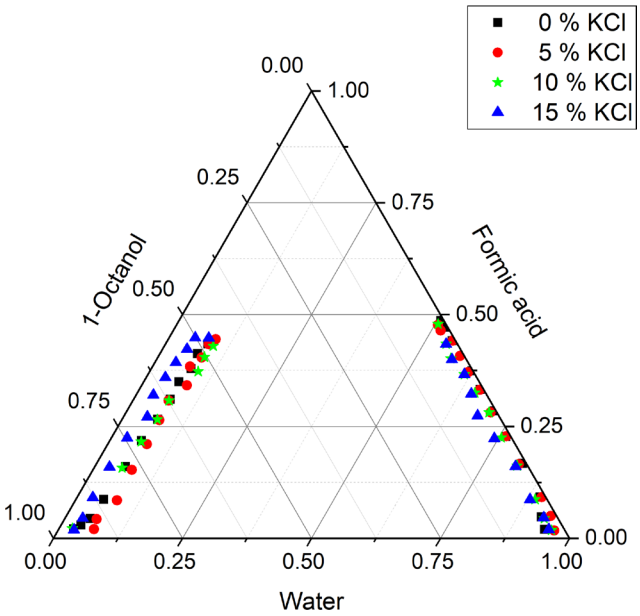

Fig. 2 Binodal curves for the system water + formic acid + 1-octanol + KCl at $T = 293.15$ K and atmospheric pressure for different KCl weight percentages (0%, 5%, 10%, and 15%)

3.1.2 Selectivity

This part introduces the concept of S in LLEx. It explains how S is calculated and its importance in evaluating the efficiency of the solvent for separating the target solute from the mixture.

Fig. 3 shows how S evolves with increasing NaCl concentration. S is defined as the ratio of FA's affinity for the organic phase relative to water. As the NaCl concentration

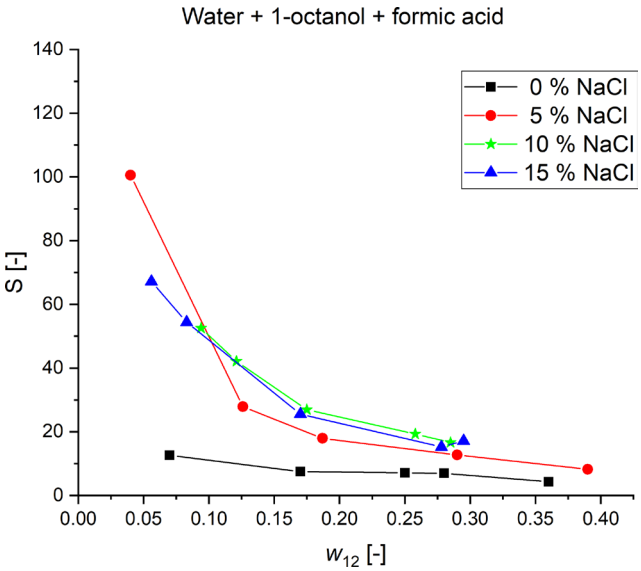

Fig. 3 Selectivity diagram for the system water + formic acid + 1-octanol + NaCl at $T = 293.15$ K and atmospheric pressure for different NaCl weight percentages (0%, 5%, 10%, and 15%)

increases from 0% to 10%, a significant improvement in S is observed due to the salting-out effect. At 15%, the increase plateaus, indicating the system approaches a saturation point in terms of enhanced extraction efficiency.

Fig. 4 presents the variation of S with KCl concentration. The S in the presence of KCl also increases with salt concentration; however, the magnitude of this improvement is lower than that observed with NaCl. This difference is attributed to the weaker hydration energy and ionic strength of K^+ compared to Na^+, resulting in a less effective salting-out mechanism.

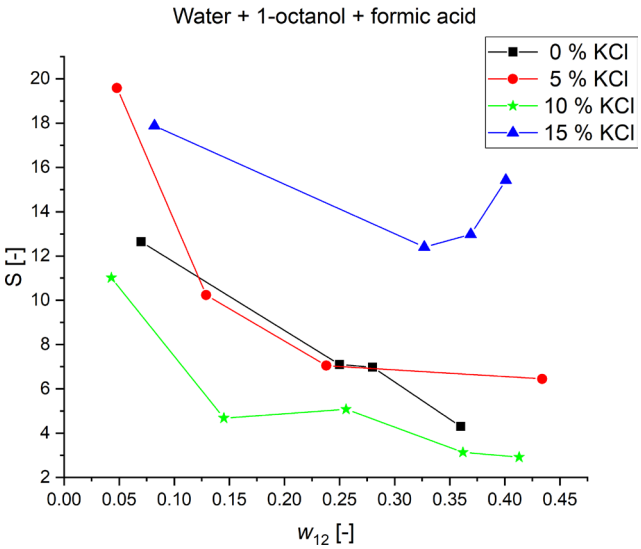

Fig. 4 Selectivity diagram for the system water + formic acid + 1-octanol + KCl at $T = 293.15$ K and atmospheric pressure for different KCl weight percentages (0%, 5%, 10%, and 15%)

3.1.3 Distribution coefficients

This part focuses on the calculation of D_2, which quantify the extent to which the solute partitions between the two phases. The methodology for determining these values from experimental data is briefly discussed.

Fig. 5 illustrates the D_2 of FA between the two phases as NaCl concentration increases. The D_2 quantifies the ratio of FA concentration in the organic phase to that in the aqueous phase. In the presence of NaCl, the coefficient increases with salt concentration, peaking around 10%, confirming NaCl's strong role in shifting FA toward the organic layer. At 15%, the curve begins to stabilize, suggesting diminishing marginal returns due to saturation effects.

Fig. 6 shows the effect of KCl concentration on the distribution of FA. The addition of KCl causes a similar but less pronounced increase in D_2. The weaker impact at 10% and 15% salt concentrations highlights the relatively lower capacity of K^+ ions to induce strong salting-out behavior, likely due to their larger ionic radius and lower charge density compared to Na^+.

The stronger salting-out effect observed with NaCl compared to KCl can be explained thermodynamically by considering ion hydration energy, ionic radius, and activity coefficients. Sodium ions possess a smaller ionic radius (0.102 nm) and therefore exhibit a higher charge density than potassium ions (0.138 nm). This higher charge density results in a stronger electrostatic attraction to water molecules, leading to a more negative hydration energy (−406 kJ mol^{-1} for Na^+ *vs.* −322 kJ mol^{-1} for K^+) [30].

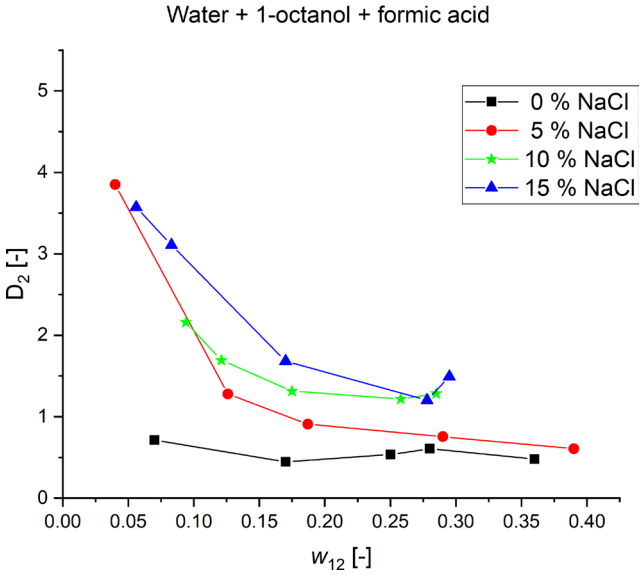

Fig. 5 Distribution coefficient of formic acid for the system water + formic acid + 1-octanol + NaCl at T = 293.15 K and atmospheric pressure for NaCl concentrations of 0%, 5%, 10%, and 15%

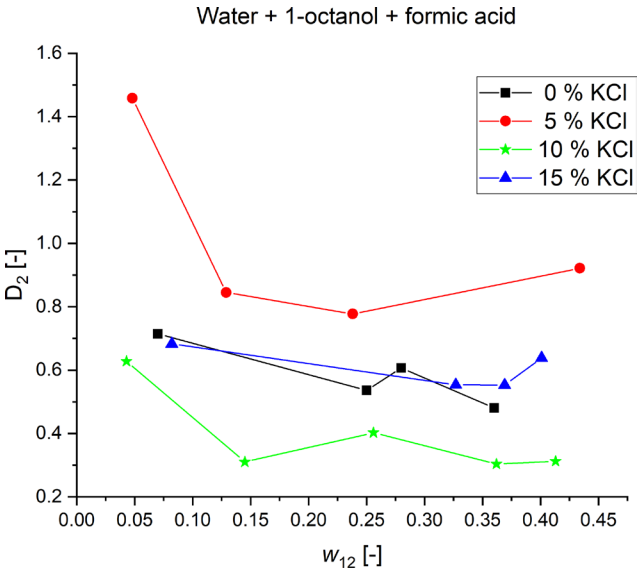

Fig. 6 Distribution coefficient of formic acid for the system water + formic acid + 1-octanol + KCl at T = 293.15 K and atmospheric pressure for KCl concentrations of 0%, 5%, 10%, and 15%

Consequently, Na^+ ions are more strongly solvated, binding water molecules tightly within their hydration shells.

3.1.4 Reliability of experimental data

The reliability and consistency of the experimentally determined LLEq data are essential for developing accurate thermodynamic models. To verify the quality of the tie-line data, two classical and widely accepted empirical correlations were employed: the Othmer–Tobias correlation [31] and the Hand correlation [32]. These correlations serve as effective diagnostic tools to assess the thermodynamic consistency of the experimental measurements, especially in ternary and quaternary systems.

The Othmer–Tobias correlation is expressed as:

$$\ln\left(\frac{(1-w_{33})}{w_{33}}\right) = a + b\ln\left(\frac{1-w_{11}}{w_{11}}\right), \tag{1}$$

where w_{11} and w_{33} are the mass fractions of the solvent and solute, respectively, in the raffinate phase. The parameters a and b are correlation coefficients obtained through linear regression.

The Hand correlation is defined by the following relationship (Eq. (2)):

$$\ln\left(\frac{w_{21}}{w_{11}}\right) = a + b\ln\left(\frac{w_{23}}{w_{33}}\right), \tag{2}$$

where w_{21} and w_{23} are the mass fractions of the solvent and solute in the extract phase, respectively, while w_{11} and w_{33} are their counterparts in the raffinate phase. Again, a and b

are empirical coefficients derived from the slope and intercept of the fitted line.

Both correlations were applied to each set of tie-line data obtained experimentally for the quaternary systems involving water, FA, 1-octanol, and salts (NaCl or KCl).

Tables 2 and 3 present the constants obtained from the Othmer–Tobias and Hand correlations for the quaternary systems (water + 1-octanol + FA + salt), specifically with NaCl and KCl, respectively, at a constant temperature of 293.15 K and atmospheric pressure. These constants include the linear regression parameters *a* and *b*, along with the coefficient of determination R^2, which indicates the quality of the linear fit. For the NaCl system (Table 1), the R^2 values for both correlations range from 0.93897 to 0.98134, confirming a strong linear relationship and high consistency of the experimental tie-line data across all salt concentrations (0%, 5%, 10%, and 15%). Similarly, for the KCl system (Table 2), the R^2 values range from 0.93178 to 0.98607, again confirming the reliability of the measurements. The slight variations in the correlation parameters with increasing salt concentration suggest subtle changes in the phase behavior due to salt-specific effects. Overall, the high R^2 values across both correlations and salt types provide strong evidence that the experimental data are thermodynamically consistent and suitable for use in modeling and predictive analysis.

3.2 NRTL modelling

The binary interaction parameters of the NRTL model were estimated based on the experimental LLEq data [33]. A comparison between the experimental tie lines and those calculated using the NRTL model is illustrated in Figs. 3 and 4. The close agreement between the two confirms the model's ability to accurately describe the phase behavior of the studied system. Parameter estimation was performed by minimizing an objective function (F) using the Particle Swarm Optimization (PSO) algorithm, implemented through MATLAB 2016a's optimization toolbox [34]. The objective F, defined as the sum of squared differences between experimental and calculated compositions across all components and tie lines, is given by:

$$\min(F) = \sum_{k=1}^{m}\sum_{j=1}^{2}\sum_{i=1}^{n} w_{ik}^{j}\left(x_{ik}^{cal}(j) - x_{ik}^{\exp}(j)\right)^2, \tag{3}$$

where $w_{ik}^{j} = 1$ for all terms. The accuracy of the model was quantified by calculating the root mean square error (RMSE) between experimental and predicted compositions [35]:

$$\mathrm{RMSE} = \left[\frac{-F}{2\ m\ n}\right]^{0.5}, \tag{4}$$

where m is the number of tie lines and n is the number of components. The RMSE values obtained for each system are reported in Table 3 and show low error values, confirming the robustness and predictive capability of the NRTL model for the studied LLEq system.

Fig. 7 illustrates the experimental liquid–liquid equilibrium phase diagram and tie-line data for the NaCl-containing system, overlaid with predictions from the NRTL model. Fig. 8 presents the corresponding data for the system with KCl. In both cases, the NRTL model shows good agreement with the experimental results, particularly at low and moderate salt concentrations. However, at higher salt concentrations (15%), noticeable deviations are observed – more prominently in the KCl system – indicating increased non-ideality due to higher ionic strength. The accurate reproduction of tie-line data across most concentrations demonstrates the reliability and robustness of the NRTL model for quaternary systems involving water,

Table 2 Constants of Othmer–Tobias and Hand correlations and regression coefficients for the water + 1-octanol + formic acid + NaCl

NaCl (%)	Othmer–Tobias correlation			Hand correlation		
	a	*b*	R^2	*a*	*b*	R^2
0	0.52627	−0.87762	0.98134	1.34872	1.31974	0.97481
5	−0.82017	0.33974	0.95724	2.6915	2.52602	0.95371
10	0.76705	0.24716	0.95504	1.51836	−0.09908	0.95065
15	0.3198	−0.15456	0.93897	0.3198	−0.09908	0.93897

Table 3 Constants of Othmer–Tobias and Hand correlations and regression coefficients for the water + 1-octanol + formic acid + KCl

KCl (%)	Othmer–Tobias correlation			Hand correlation		
	a	*b*	R^2	*a*	*b*	R^2
5	0.35239	−0.8707	0.93178	1.16123	0.24854	0.93332
10	0.44836	−1.33869	0.95016	1.48386	2.36144	0.9503
15	0.72095	−0.82063	0.98171	0.60989	0.26267	0.98607

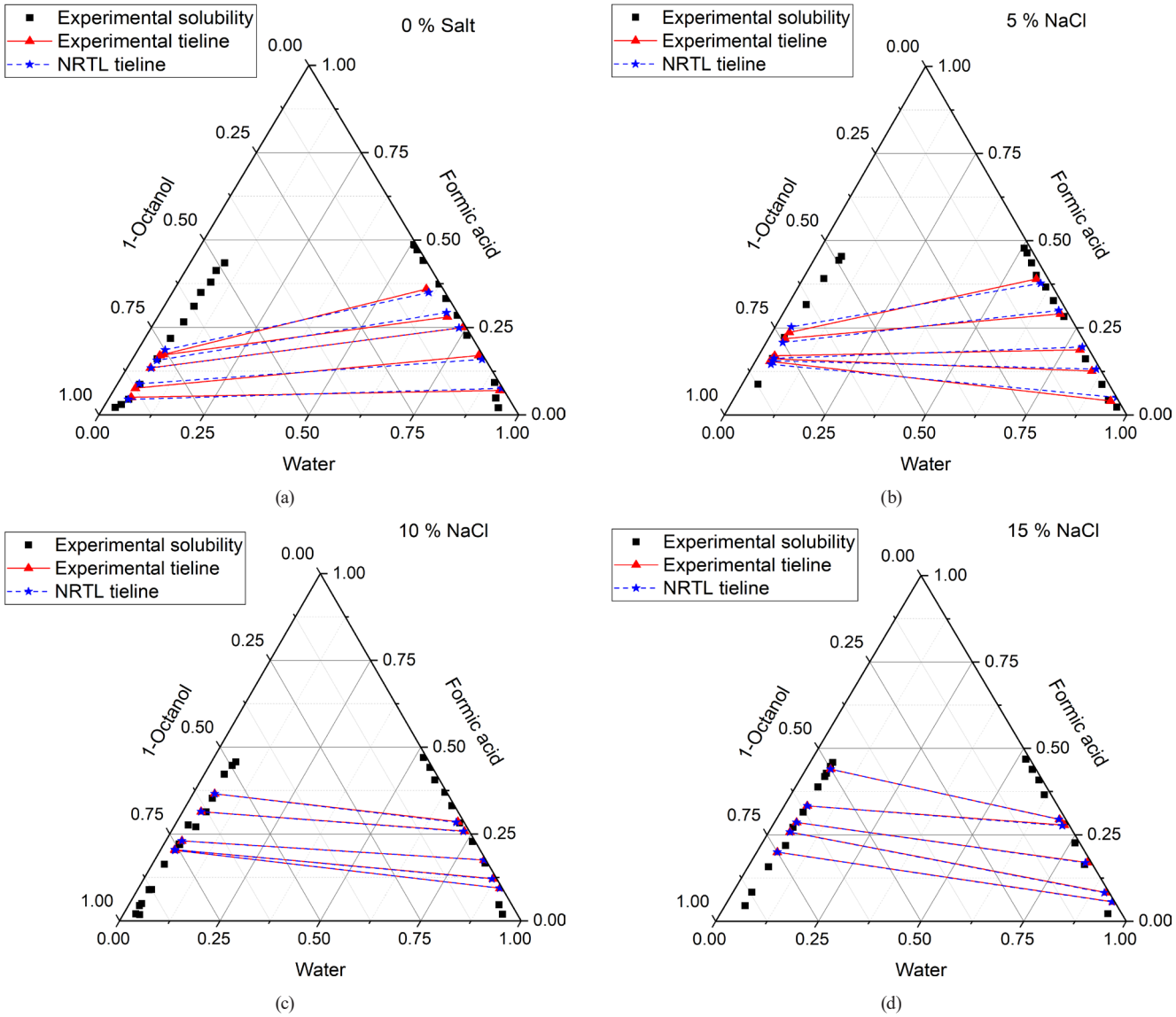

Fig. 7 Experimental and NRTL-calculated tie lines for the system water + formic acid + 1-octanol + NaCl at $T = 293.15$ K and atmospheric pressure for NaCl concentrations of 0%, 5%, 10%, and 15%: (a) 0% NaCl; (b) 5% NaCl; (c) 10% NaCl; (d) 15% NaCl

organic solvents, and inorganic salts. The discrepancies observed at higher salt levels underscore the potential limitations of the current parameter set and suggest the need for incorporating salt-specific interaction terms or extending the model with electrolyte corrections in future studies.

Table 4 presents the binary interaction parameters A_{ij} and A_{ji} of the NRTL model along with the corresponding RMSE values for the quaternary system water + 1-octanol + FA under various salt concentrations. These parameters were estimated using the PSO algorithm to minimize the deviation between experimental and calculated compositions. The RMSE values indicate the quality of the model fit, with lower RMSE suggesting better agreement. Notably, the model achieved its best performance at 5% KCl concentration (RMSE = 0.0522), followed by 10% NaCl (RMSE = 0.1283), highlighting the influence of salt type and concentration on model accuracy. For systems without salt or at higher concentrations (e.g., 15% KCl or 10% KCl), the RMSE values increased slightly, suggesting that non-ideal behavior becomes more pronounced at elevated ionic strengths. Overall, the optimized parameters provide reliable inputs for phase equilibrium prediction and validate the applicability of the NRTL model for complex quaternary systems involving electrolytes.

Tables 5 and 6 present the experimental tie-line data, the corresponding predictions from the NRTL model, the objective F, and the root mean square deviation (RMSE) values for both the NaCl and KCl systems at various salt concentrations (0%, 5%, 10%, and 15%).

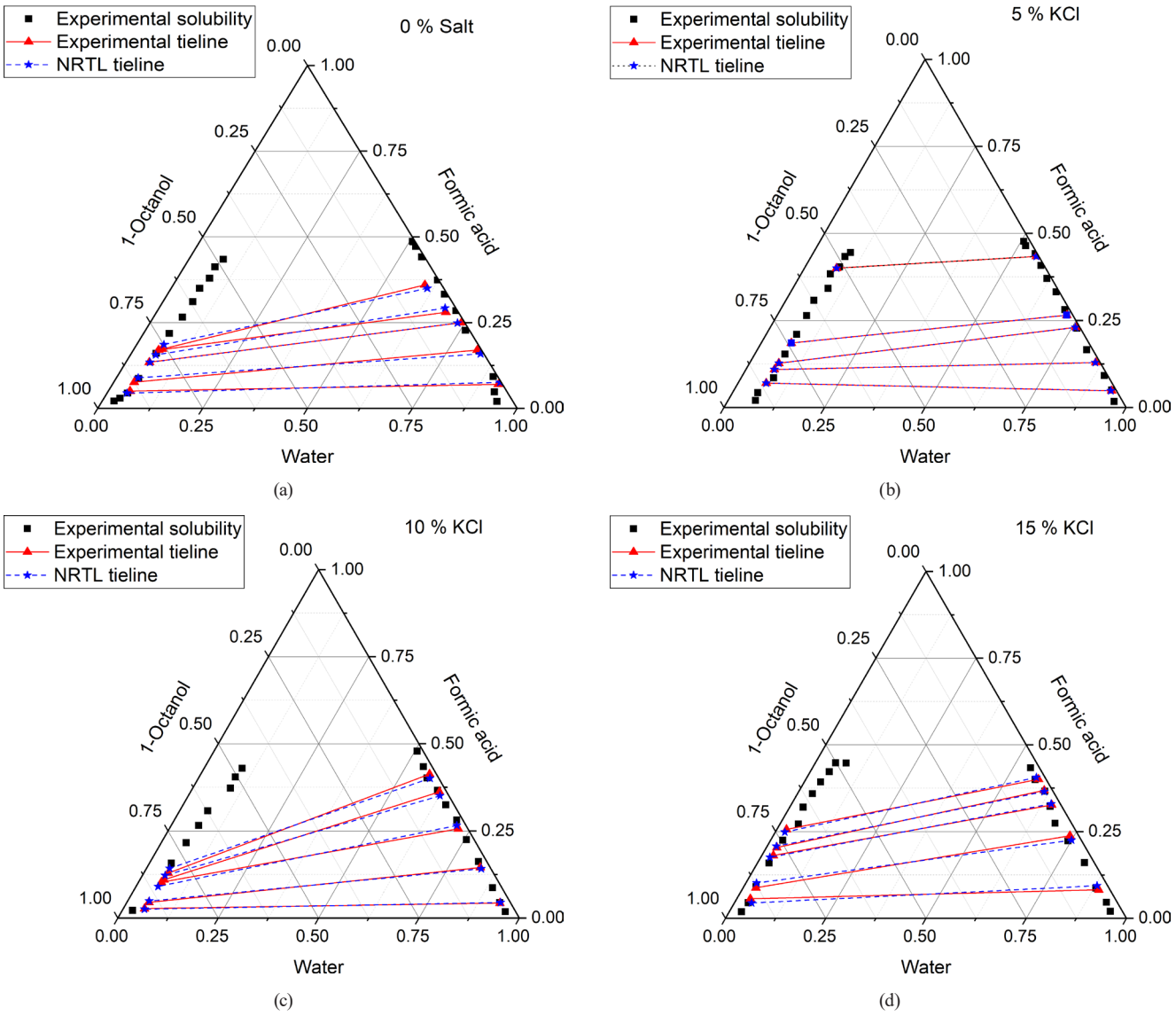

Fig. 8 Experimental and NRTL-calculated tie lines for the system water + formic acid + 1-octanol + KCl at T = 293.15 K and atmospheric pressure for KCl concentrations of 0%, 5%, 10%, and 15%: (a) 0% KCl; (b) 5% KCl; (c) 10% KCl; (d) 15% KCl

For the NaCl system (Table 5), the NRTL model shows excellent agreement with the experimental data across all salt concentrations. At 0% salt, the model yielded an RMSE of 0.8113, indicating a reliable prediction of equilibrium compositions in the ternary base system. As the salt concentration increased to 5% and 10%, the model maintained high accuracy with RMSE values of 0.5568 and 0.1283, respectively. This trend highlights the model's robustness under moderate ionic strength. At 15% salt, the RMSE slightly increased to 0.1829, which is still acceptable but suggests a marginal decline in predictive performance at higher ionic strengths, likely due to enhanced non-ideal behavior in the system.

For the KCl system (Table 6), a similar pattern is observed. At 5% salt, the NRTL model captures the tie-line data with an RMSE of 0.0522, reflecting very accurate predictions. With increasing salt concentrations (10% and 15%), RMSE values were 0.7178 and 0.7095, respectively. Although these values are slightly higher compared to lower salt concentrations, the model still demonstrates a reasonable ability to reproduce the experimental equilibrium data. Deviations become more apparent at 15% KCl, which may be attributed to specific ion effects or stronger ionic interactions not accounted for in the standard NRTL parameterization. The deviations observed at 15% salt concentration are mainly due to the increased ionic strength and specific ion–solute interactions not captured by the standard NRTL model. In this study, the NRTL interaction parameters were estimated on a salt-free basis [36], which assumes that salt effects are implicitly included through changes in the overall composition rather than explicit ion–solvent interactions.

Table 4 RMSE and NRTL binary interaction parameters values for (water + 1-octanol + formic acid)

Concentration	*i–j*	A_{ij}	A_{ji}
	1–2	12.1008	9.4018
0% salt	1–3	15.5000	9.0708
	2–3	4.1972	16.1336
	1–2	3.6606	20.6431
5% NaCl	1–3	12.9934	3.7596
	2–3	16.7004	4.8983
	1–2	12.0161	14.6300
10% NaCl	1–3	3.2036	−13.7100
	2–3	5.9371	−6.6411
	1–2	2.6512	−1.7315
15% NaCl	1–3	13.1300	−12.2200
	2–3	−2.9758	0.0204
	1–2	30.7600	25.9351
5% KCl	1–3	30.7600	−18.9654
	2–3	11.3819	−21.9623
	1–2	14.7015	47.7529
10% KCl	1–3	3.9569	10.9825
	2–3	3.8171	44.5060
	1–2	−1.6341	10.3282
15% KCl	1–3	11.7614	8.6165
	2–3	15.3602	20.7505

At high salt levels, however, this assumption becomes less valid because strong electrostatic and hydration effects significantly alter solvent activity and local composition, leading to noticeable discrepancies between experimental and predicted values. Incorporating electrolyte-specific corrections, such as those used in electrolyte non-random two-liquid (eNRTL) or Pitzer models, could therefore improve accuracy under high ionic strength conditions.

3.3 ANN modelling

The ANN was implemented in MATLAB [34] and trained on experimental data to capture the nonlinear relationship between the feed composition, salt concentration, and the resulting mass fractions of the components in both the extract and raffinate phases. Six input variables were selected, including the mass fractions of the three components in the feed, salt concentration, and solubility parameters, while the outputs corresponded to the mass fractions of the same components in each equilibrium phase. The network was trained using the Levenberg–Marquardt algorithm, and the dataset was divided into training (70%), validation (15%), and testing (15%) subsets to ensure accurate generalization [24]. Model performance was assessed using mean squared error (MSE), demonstrating that the ANN could reliably reproduce experimental data and predict phase compositions across varying salt concentrations.

To determine the optimal ANN architecture, a NAS approach was used. This method performed a grid-based exploration of different network structures by varying key hyperparameters, including the number of neurons in the first and second hidden layers (ranging from 1 to 15), and the type of activation functions used in each layer [37]. The tested activation functions included the log-sigmoid, tangent-sigmoid, and pure linear functions [17]. Additionally, a 5-fold cross-validation was also performed to evaluate the robustness and generalization of the ANN model. The optimal network structure obtained through this search comprised 6 input neurons, two hidden layers with 10 and 8 neurons respectively, and a single output neuron. The log-sigmoid function was used in the first hidden layer, while the tangent-sigmoid function was selected for the second. This configuration showed the best predictive performance and stability across training, validation, and test data. Table 7 presents the input and target data employed to train, validate, and test the ANN model for predicting the phase compositions in the LLEq system.

Fig. 9 presents the regression plots for both the ANN and NRTL models based on the combined training, validation, and testing datasets. The ANN model exhibits

Table 5 Experimental tie-line data, NRTL calculated points, RMSE and objective function for (water with NaCL+ 1-octanol + formic acid) system

0% NaCl formic acid							
Experimental						*F*	RMSE
0.9200	0.0700	0.0100	0.0520	0.0500	0.8980		
0.8200	0.1700	0.0100	0.0490	0.0760	0.8750		
0.7420	0.2500	0.0080	0.0560	0.1340	0.8100		
0.6900	0.2800	0.0300	0.0600	0.1700	0.7700		
0.6000	0.3600	0.0400	0.0670	0.1730	0.7600		
NRTL						0.0020	0.8113
0.9191	0.0695	0.0114	0.0515	0.0504	0.8981		
0.8213	0.1644	0.0143	0.0538	0.0823	0.864		
0.7386	0.2556	0.0059	0.0576	0.1281	0.8144		
0.679	0.2941	0.0269	0.0598	0.1534	0.7868		
0.6144	0.3478	0.0378	0.0633	0.1883	0.7484		
5%							
Experimental						*F*	RMSE
0.9400	0.0400	0.0200	0.0360	0.1540	0.8100		
0.8500	0.1260	0.0240	0.0390	0.1610	0.8000		
0.7900	0.1870	0.0230	0.0400	0.1700	0.7900		
0.6900	0.2900	0.0200	0.0410	0.2190	0.7400		
0.5800	0.3900	0.0300	0.0430	0.2370	0.7200		
NRTL						9.300e-04	0.5568
0.9341	0.041	0.0249	0.0417	0.153	0.8054		
0.8404	0.1352	0.0244	0.0434	0.1519	0.8047		
0.7951	0.1809	0.024	0.0409	0.1762	0.783		
0.6926	0.2843	0.0231	0.0367	0.2245	0.7388		
0.5853	0.3927	0.022	0.036	0.2338	0.7302		
10%							
Experimental						*F*	RMSE
0.9000	0.0940	0.0060	0.0370	0.2030	0.7600		
0.8700	0.1210	0.0090	0.0350	0.2050	0.7600		
0.8200	0.1750	0.0050	0.0400	0.2300	0.7300		
0.7300	0.2580	0.0120	0.0460	0.3140	0.6400		
0.7000	0.2850	0.0150	0.0540	0.3660	0.5800		
NRTL						4.938e-05	0.1283
0.9000	0.0940	0.0060	0.0370	0.2030	0.7600		
0.8700	0.1210	0.0123	0.0350	0.2050	0.7600		
0.8200	0.1750	0.0050	0.0400	0.2300	0.7300		
0.7299	0.2580	0.0153	0.0460	0.3140	0.6400		
0.6999	0.2850	0.0202	0.0540	0.3660	0.5800		

Table 5 Experimental tie-line data, NRTL calculated points, RMSE and objective function for (water with NaCL+ 1-octanol + formic acid) system (continued)

15%							
Experimental						*F*	RMSE
0.9400	0.0560	0.0040	0.0500	0.2000	0.7500		
0.9100	0.0830	0.0070	0.0520	0.2580	0.6900		
0.8200	0.1700	0.0100	0.0540	0.2860	0.6600		
0.7100	0.2780	0.0120	0.0560	0.3340	0.6100		
0.6900	0.2950	0.0150	0.0600	0.4400	0.5000		
NRTL						1.003e-04	0.1829
0.9400	0.0561	0.0073	0.0500	0.2000	0.7500		
0.9099	0.0831	0.0122	0.0520	0.2580	0.6900		
0.8199	0.1701	0.0152	0.0540	0.2860	0.6600		
0.7099	0.2781	0.0176	0.0560	0.3340	0.6100		
0.6900	0.2950	0.0168	0.0600	0.4400	0.5000		

Table 6 Experimental tie-line data, NRTL calculated points, RMSD and objective function for (water with KCL+ 1-octanol + formic acid) system

5% KCl formic acid							
Experimental						*F*	RMSE
0.9400	0.04800	0.0120	0.0700	0.0700	0.8600		
0.8600	0.1290	0.0110	0.0710	0.1090	0.8200		
0.7600	0.2300	0.0100	0.0730	0.1270	0.800		
0.7200	0.2650	0.0150	0.0750	0.1850	0.7400		
0.5600	0.4340	0.006	0.080	0.4000	0.5200		
NRTL						8.164e-06	0.0522
0.9400	0.0480	0.0141	0.0700	0.0700	0.8600		
0.8600	0.1290	0.0123	0.0710	0.1090	0.8200		
0.7600	0.2300	0.0113	0.0730	0.1270	0.800		
0.7200	0.2650	0.0155	0.0750	0.1850	0.7400		
0.5600	0.4340	0.0060	0.0800	0.4000	0.5200		
10%							
Experimental						*F*	RMSE
0.9300	0.0430	0.0270	0.0530	0.0270	0.9200		
0.8300	0.1450	0.0250	0.0550	0.0450	0.9000		
0.7200	0.2560	0.0240	0.0570	0.1030	0.8400		
0.6200	0.3620	0.0180	0.0600	0.1100	0.8300		
0.5700	0.4130	0.0170	0.0610	0.1290	0.8100		
NRTL						0.0015	0.7178
0.931	0.0444	0.0246	0.0537	0.0256	0.9207		
0.8344	0.1416	0.0241	0.0538	0.0488	0.8974		
0.7114	0.2656	0.023	0.0549	0.0905	0.8545		
0.6268	0.3509	0.0223	0.0564	0.1224	0.8212		
0.5769	0.4013	0.0218	0.0577	0.1425	0.7997		

Table 6 Experimental tie-line data, NRTL calculated points, RMSD and objective function for (water with KCL+ 1-octanol + formic acid) system (continued)

15%							
Experimental						*F*	RMSE
0.8900	0.0820	0.0280	0.0340	0.0560	0.9100		
0.7400	0.2380	0.0220	0.0320	0.0880	0.8800		
0.6500	0.3270	0.0230	0.0290	0.1810	0.7900		
0.6100	0.3690	0.0210	0.0260	0.2040	0.7700		
NRTL						0.0015	0.7095
0.8797	0.0938	0.0264	0.0432	0.0441	0.9127		
0.7505	0.2252	0.0243	0.0266	0.1016	0.8718		
0.6473	0.3299	0.0228	0.0229	0.1759	0.8013		
0.6124	0.3653	0.0223	0.023	0.2076	0.7694		

Table 7 Input and output variables used in ANN model

Input	Output
Mass fractions in the feed: w_{01}, w_{02} and w_{03} Salt concentration Solubility of salt in water	Mass fractions of components in each phase at equilibrium: w_{11}, w_{12}, w_{13}, w_{21}, w_{22} and w_{23}

an almost perfect linear relationship between the predicted and experimental values, with a correlation coefficient of R = 0.99985, confirming its outstanding predictive accuracy. In contrast, the NRTL model shows a slightly lower correlation (R = 0.9997), indicating less precision in reproducing experimental data.

The close alignment of ANN-predicted values with experimental compositions and the minimal data dispersion around the regression line demonstrate the network's ability to capture the nonlinear dependencies among feed composition, salt concentration, and solubility parameters. Additionally, the small residual errors observed across all subsets confirm that the ANN generalized effectively without overfitting.

These findings validate both the reliability of the Neural Architecture Search-optimized ANN and its superior predictive capability compared to the classical NRTL model. Consequently, the ANN model provides a more accurate and robust tool for predicting equilibrium compositions in electrolyte-assisted LLEq systems.

To strengthen the validation of the proposed models, several statistical performance indicators were evaluated, including the Mean Absolute Error, Mean Squared Error, Root Mean Squared Error, Mean Absolute Percentage Error, and the coefficient of determination.

As presented in Table 8, the ANN model exhibits superior performance compared to the NRTL model. The ANN produced significantly lower error values (MAE = 0.0031,

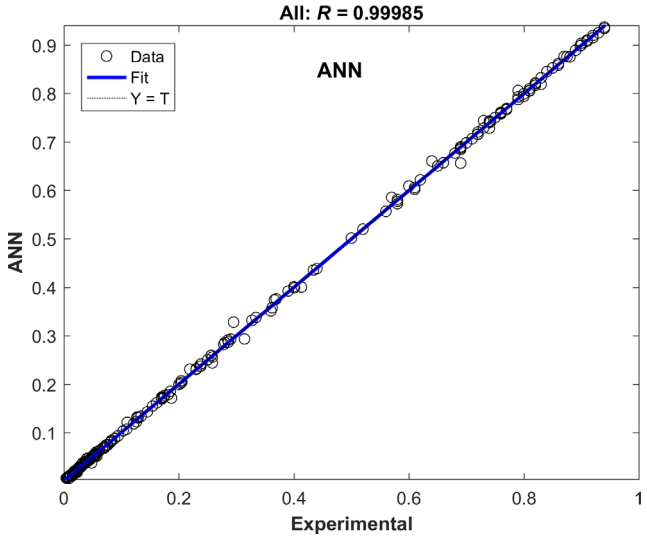

(a)

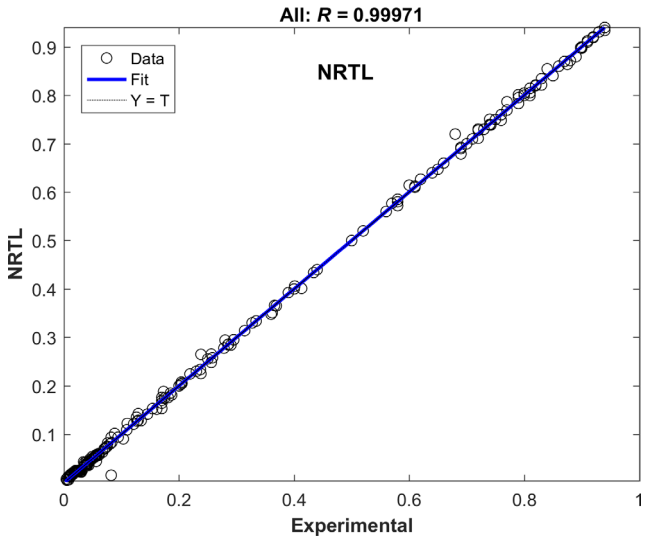

(b)

Fig. 9 Regression analysis of artificial neural network for training, testing, and validation data and NRTL for the water + formic acid + 1-octanol + salt (NaCl or KCl) system: (a) ANN; (b) NRTL

Table 8 Statistical performance metrics of the ANN and NRTL models for predicting the phase behavior of the water + formic acid + 1-octanol system with salts (NaCl and KCl)

Model	MAE	MSE	RMSE	MAPE (%)	R^2	R
ANN	0.0031188	3.1555×10^{-5}	0.0056173	3.2692	0.9997	0.99985
NRTL	0.0040171	6.1254×10^{-5}	0.0078265	5.7129	0.99942	0.99971

RMSE = 0.0056, MAPE = 3.27%) than the NRTL model (MAE = 0.0040, RMSE = 0.0078, MAPE = 5.71%). The coefficient of determination (R^2) of 0.9997 for the ANN model indicates an almost perfect correlation between predicted and experimental compositions, confirming its strong predictive accuracy and generalization capability.

The results demonstrate that the ANN model can effectively capture nonlinear relationships between phase compositions and salt concentration, which are often difficult to describe using conventional thermodynamic models such as NRTL. Moreover, the small residuals and low prediction errors confirm that the ANN can reproduce experimental tie-line data with excellent precision across both NaCl and KCl systems. These findings validate the robustness of the ANN framework as a reliable alternative or complementary approach to traditional thermodynamic modeling for predicting liquid–liquid equilibrium in multi-component and electrolyte systems.

Fig. 10 illustrates the residuals between the predicted values obtained from the ANN and NRTL models and the corresponding experimental data. The residuals are computed as the difference between the predicted and experimental values, providing a quantitative measure of model performance. This analysis reveals the practical strengths of both modeling approaches.

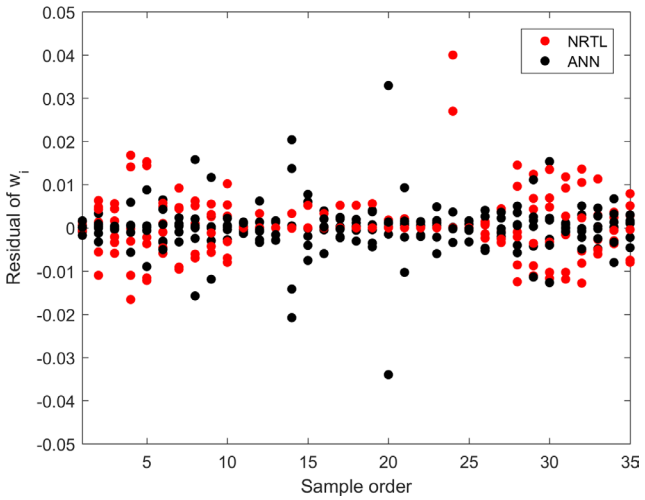

Fig. 10 Comparison of residuals between ANN and NRTL models with experimental data for the water + formic acid + 1-octanol + salt (NaCl and KCl) system

4 Conclusion

This study presents an integrated experimental and modeling investigation of the liquid–liquid equilibrium behavior in quaternary systems comprising water, FA, 1-octanol, and varying concentrations (0–15%) of NaCl and KCl. Experimental solubility and tie-line data were generated under atmospheric pressure to assess the influence of salt type and concentration on extraction performance. The results confirmed that NaCl induces a stronger salting-out effect than KCl, significantly enhancing phase separation and improving extraction efficiency particularly at 10% concentration, where the highest S and D_2 were observed.

Thermodynamic modeling using the NRTL model, optimized *via* PSO, demonstrated strong agreement with experimental data at low to moderate salt levels. However, deviations at higher concentrations indicate increased non-ideality and limitations in NRTL's applicability under high ionic strength conditions.

In contrast, the ANN model optimized through NAS exhibited higher predictive accuracy and better generalization, with an excellent correlation coefficient (R = 0.99985) and lower error values compared to the NRTL model. The ANN effectively captured the complex nonlinear dependencies between system composition and phase behavior, especially in the presence of electrolytes.

Overall, this work demonstrates that the ANN model outperforms the traditional NRTL approach in predicting the phase behavior of electrolyte-assisted LLEq systems. The combination of experimental data, thermodynamic modeling, and advanced machine learning provides a robust and versatile framework for understanding and optimizing extraction processes involving carboxylic acids and inorganic salts.

Acknowledgment

The authors gratefully acknowledge the financial support provided by the Algerian Directorate General for Scientific Research and Technological Development (DGRSDT).

References

[1] Treybal, R. E. "Mass-transfer operations", McGraw-Hill, Inc., 1980. ISBN 0-07-065176-0

[2] Sørensen, J. M., Magnussen, T., Rasmussen, P., Fredenslund, A. "Liquid-liquid equilibrium data: Their retrieval, correlation and prediction Part I: Retrieval", Fluid Phase Equilibria, 2(4), pp. 297–309, 1979. https://doi.org/10.1016/0378-3812(79)80015-1

[3] Laitinen, A. T., Parsana, V. M., Jauhiainen, O., Huotari, M., van den Broeke, L. J. P., de Jong, W., Vlugt, T. J. H., Ramdin, M. "Liquid–Liquid Extraction of Formic Acid with 2-Methyltetrahydrofuran: Experiments, Process Modeling, and Economics", Industrial & Engineering Chemistry Research, 60(15), pp. 5588–5599, 2021. https://doi.org/10.1021/acs.iecr.1c00159

[4] Hong, Y. K., Hong, W. H., Chang, Y. K. "Effect of pH on the extraction characteristics of succinic and formic acids with tri-n-octylamine dissolved in 1-octanol", Biotechnology and Bioprocess Engineering, 6(5), pp. 347–351, 2001. https://doi.org/10.1007/BF02933004

[5] Senol, A. "Liquid–liquid equilibria for ternary systems of (water + carboxylic acid + 1-octanol) at 293.15 K: modeling phase equilibria using a solvatochromic approach", Fluid Phase Equilibria, 227(1), pp. 87–96, 2005. https://doi.org/10.1016/j.fluid.2004.10.029

[6] Gilani, H. G., Asan, S. "Liquid–liquid equilibrium data for systems containing of formic acid, water, and primary normal alcohols at T = 298.2 K", Fluid Phase Equilibria, 354, pp. 24–28, 2013. https://doi.org/10.1016/j.fluid.2013.06.006

[7] Reichardt, C., Welton, T. "Solvents and Solvent Effects in Organic Chemistry", Wiley-VCH Verlag GmbH & Co. KGaA, 2010. ISBN 978-3-527-32473-6 https://doi.org/10.1002/9783527632220

[8] Guerin, G., Bellocq, A. M. "Effect of salt on the phase behavior of the ternary system water-pentanol-sodium dodecylsulfate", The Journal of Physical Chemistry, 92(9), pp. 2550–2557, 1988. https://doi.org/10.1021/j100320a031

[9] Santos, F. S., d'Ávila, S. G., Aznar, M. "Salt effect on liquid–liquid equilibrium of water+1-butanol+acetone system: experimental determination and thermodynamic modeling", Fluid Phase Equilibria, 187–188, pp. 265–274, 2001. https://doi.org/10.1016/S0378-3812(01)00541-6

[10] Fu, H., Sun, Y., Teng, H., Zhang, D., Xiu, Z. "Salting-out extraction of carboxylic acids", Separation and Purification Technology, 139, pp. 36–42, 2015. https://doi.org/10.1016/j.seppur.2014.11.001

[11] Sørensen, J. M., Magnussen, T., Rasmussen, P., Fredenslund, A. "Liquid—liquid equilibrium data: Their retrieval, correlation and prediction Part II: Correlation", Fluid Phase Equilibria, 3(1), pp. 47–82, 1979. https://doi.org/10.1016/0378-3812(79)80027-8

[12] Heidemann, R. A., Mandhane, J. M. "Some properties of the NRTL equation in correlating liquid—liquid equilibrium data", Chemical Engineering Science, 28(5), pp. 1213–1221, 1973. https://doi.org/10.1016/0009-2509(73)85030-4

[13] Himmelblau, D. M. "Accounts of Experiences in the Application of Artificial Neural Networks in Chemical Engineering", Industrial & Engineering Chemistry Research, 47(16), pp. 5782–5796, 2008. https://doi.org/10.1021/ie800076s

[14] Venkatasubramanian, V. "The promise of artificial intelligence in chemical engineering: Is it here, finally?", AIChE Journal, 65(2), pp. 466–478, 2019. https://doi.org/10.1002/aic.16489

[15] Hoskins, J. C., Himmelblau, D. M. "Artificial neural network models of knowledge representation in chemical engineering", 12(9–10), pp. 881–890, 1988. https://doi.org/10.1016/0098-1354(88)87015-7

[16] Elsken, T., Metzen, J. H., Hutter, F. "Neural Architecture Search: A Survey", Journal of Machine Learning Research, 20(55), pp. 1–21, 2019. [online] Available at: https://www.jmlr.org/papers/volume20/18-598/18-598.pdf [Accessed: 15 September 2025]

[17] Athmani, K., Almeasar, K. S., Atiki, E., Habal, A. H. Y., Taallah, B., Guettala, A. "Machine learning methods for predicting the durability behavior of earth mortars with date palm ash", Asian Journal of Civil Engineering, 26(8), pp. 3211–3231, 2025. https://doi.org/10.1007/s42107-025-01365-0

[18] Torrecilla, J. S., Deetlefs, M., Seddon, K. R., Rodríguez, F. "Estimation of ternary liquid–liquid equilibria for arene/alkane/ionic liquid mixtures using neural networks", Physical Chemistry Chemical Physics, 10(33), pp. 5114–5120, 2008. https://doi.org/10.1039/B719533H

[19] Guo, B., Cheng, Z., Hu, S. "Neural network-based prediction of auto-ignition temperature of ternary mixed liquids", Heliyon, 10(7), e28713, 2024. https://doi.org/10.1016/j.heliyon.2024.e28713

[20] Shu, Y., Du, L., Lei, Y., Hu, S., Kuang, Y., Fang, H., Liu, X., Chen, Y. "Modeling Study on Heat Capacity, Viscosity, and Density of Ionic Liquid–Organic Solvent–Organic Solvent Ternary Mixtures via Machine Learning", Processes, 12(7), 1420, 2024. https://doi.org/10.3390/pr12071420

[21] Li, L., Jing, H., Liu, J., Pan, H., Fang, Z., Kuang, T., Lan, Y., Guo, J. "The artificial neural network-based two-phase equilibrium calculation framework for fast compositional reservoir simulation of CO_2 EOR", Fluid Phase Equilibria, 585, 114151, 2024. https://doi.org/10.1016/j.fluid.2024.114151

[22] Moghadam, M., Asgharzadeh, S. "On the application of artificial neural network for modeling liquid-liquid equilibrium", Journal of Molecular Liquids, 220, pp. 339–345, 2016. https://doi.org/10.1016/j.molliq.2016.04.098

[23] Argatov, I., Kocherbitov, V. "A note on artificial neural network modeling of vapor-liquid equilibrium in multicomponent mixtures", Fluid Phase Equilibria, 502, 112282, 2019. https://doi.org/10.1016/j.fluid.2019.112282

[24] Laiadi, C., Lami, N., Merzougui, A., Laouini, S. E. "The influence of cation and temperature on the liquid–liquid equilibrium of water + 2-butanone system and its simulation using artificial intelligent-based models", Desalination and Water Treatment, 222, pp. 196–208, 2021.
https://doi.org/10.5004/dwt.2021.27095

[25] Dean, J. A. "Lange"s Handbook of Chemistry", McGraw-Hill, Inc., 1999. ISBN 0-07-016384-7 [online] Available at: http://elibrary.bsu.edu.az/files/books_400/N_139.pdf [Accessed: 15 September 2025]

[26] Briggs, S. W., Comings, E. W. "Effect of Temperature on Liquid-Liquid Equilibrium", Industrial & Engineering Chemistry, 35(4), pp. 411–417, 1943.
https://doi.org/10.1021/ie50400a006

[27] Letcher, T. M., Ravindran, S., Radloff, S. "Liquid-liquid equilibria for mixtures of an alkanol + diisopropyl ether + water at 25°C", Fluid Phase Equilibria, 71(1–2), pp. 177–188, 1992.
https://doi.org/10.1016/0378-3812(92)85012-W

[28] Bacha, O., Hasseine, A., Attarakih, M. "Measurement and correlation of liquid–liquid equilibria for water + ethanol + mixed solvents (dichloromethane or chloroform + diethyl ether) at T = 293.15 K", Physics and Chemistry of Liquids, 54(2), pp. 245–257, 2016.
https://doi.org/10.1080/00319104.2015.1079193

[29] Laiadi, D., Hasseine, A., Merzougui, A. "Homotopy method to predict liquid–liquid equilibria for ternary mixtures of (water + carboxylic acid + organic solvent)", Fluid Phase Equilibria, 313, pp. 114–120, 2012.
https://doi.org/10.1016/j.fluid.2011.09.034

[30] Hasseine, A., Kabouche, A., Meniai, A.-H., Korichi, M. "Salting effect of NaCl and KCl on the liquid–liquid equilibria of water + ethyl acetate + ethanol system and interaction parameters estimation using the genetic algorithm", Desalination and Water Treatment, 29(1–3), pp. 47–55, 2011.
https://doi.org/10.5004/dwt.2011.1621

[31] Othmer, D., Tobias, P. "Liquid-Liquid Extraction Data - The Line Correlation", Industrial & Engineering Chemistry, 34(6), pp. 693–696, 1942.
https://doi.org/10.1021/ie50390a600

[32] Hand, D. B. "Dineric Distribution", The Journal of Physical Chemistry, 34(9), pp. 1961–2000, 1930.
https://doi.org/10.1021/j150315a009

[33] Renon, H., Prausnitz, J. M. "Local compositions in thermodynamic excess functions for liquid mixtures", AIChE Journal, 14(1), pp. 135–144, 1968.
https://doi.org/10.1002/aic.690140124

[34] The MathWorks, Inc. "MATLAB, (2016a)", [computer program] Available at: https://www.mathworks.com/downloads/web_downloads/download_release?release=R2016a [Accessed: 15 September 2025]

[35] Teh, Y. S., Rangaiah, G. P. "A Study of Equation-Solving and Gibbs Free Energy Minimization Methods for Phase Equilibrium Calculations", Chemical Engineering Research and Design, 80(7), pp. 745–759, 2002.
https://doi.org/10.1205/026387602320776821

[36] Chaouch, L. B., Merzougui, A., Laiadi, C., Bouredji, H. "Influence of salt on tie-line behavior for ternary (water + phenol + 2-butanol) system: experimental data and correlation", Desalination and Water Treatment, 259, pp. 98–106, 2022.
https://doi.org/10.5004/dwt.2022.28465

[37] Yu, K., Sciuto, C., Jaggi, M., Musat, C., Salzmann, M. "Evaluating the Search Phase of Neural Architecture Search", [preprint] arXiv, arXiv:1902.08142, 22 November 2019.
https://doi.org/10.48550/arXiv.1902.08142